Archival Report

Biological Psychiatry: CNNI

Social Buffering of Posttraumatic Stress Disorder: Longitudinal Effects and Neural Mediators

Justin L.C. Santos, Nathaniel G. Harnett, Sanne J.H. van Rooij, Timothy D. Ely, Tanja Jovanovic, Lauren A.M. Lebois, Francesca L. Beaudoin, Xinming An, Thomas C. Neylan, Sarah D. Linnstaedt, Laura T. Germine, Kenneth A. Bollen, Scott L. Rauch, John P. Haran, Alan B. Storrow, Christopher Lewandowski, Paul I. Musey Jr., Phyllis L. Hendry, Sophia Sheikh, Christopher W. Jones, Brittany E. Punches, Jose L. Pascual, Mark J. Seamon, Erica Harris, Claire Pearson, David A. Peak, Roland C. Merchant, Robert M. Domeier, Niels K. Rathlev, Brian J. O'Neil, Paulina Sergot, Leon D. Sanchez, Steven E. Bruce, Diego A. Pizzagalli, Steven E. Harte, Kerry J. Ressler, Karestan C. Koenen, Samuel A. McLean, and Jennifer S. Stevens

ABSTRACT

BACKGROUND: Posttraumatic stress disorder (PTSD) is a well-characterized psychiatric disorder that features changes in mood and arousal following traumatic events. Previous animal and human studies of social support during the peritraumatic window have demonstrated a buffering effect with regard to acute biological and psychological stress symptoms. Fewer studies have explored the magnitude of and mechanism through which early posttrauma social support can reduce longitudinal PTSD severity.

METHODS: In this study, we investigated the beneficial impact of social support on longitudinal PTSD symptoms and probed brain regions sensitive to this buffering phenomenon, such as the amygdala and ventromedial prefrontal cortex. In the multisite AURORA study, 315 participants reported PTSD symptoms (PTSD Checklist for DSM-5) and perceived emotional support (Patient-Reported Outcomes Measurement Information System) at 2 weeks, 8 weeks, 3 months, and 6 months post emergency department visit. Additionally, neuroimaging data were collected at 2 weeks posttrauma.

RESULTS: We hypothesized that early posttrauma social support would be linked with greater fractional anisotropic values in white matter tracts that have known connectivity between the amygdala and prefrontal cortex and would predict reduced neural reactivity to social threat cues in the amygdala. Interestingly, while we observed greater fractional anisotropy in the bilateral cingulum and bilateral uncinate fasciculus as a function of early posttrauma emotional support, we also identified greater threat reactivity in the precuneus/posterior cingulate, a component of the default mode network.

CONCLUSIONS: Our findings suggest that the neurocircuitry underlying the response to social threat cues is facilitated through broader pathways that involve the posterior hub of the default mode network.

https://doi.org/10.1016/j.bpsc.2024.11.011

Posttraumatic stress disorder (PTSD) affects approximately 8% of the general population in the United States (1,2). Various models suggest both biological and psychological vulnerability components to risk for PTSD (1,3). However, meta-analyses have found that a lack of social support is at the top of the list of predictive risk factors for PTSD, accounting for 16% of the variance (3–5). Universal to all traumas, social isolation exacerbates PTSD symptom severity (6–8). In the current study, we investigated neural mechanisms by which early posttrauma social support may reduce longitudinal posttraumatic stress symptoms, thereby promoting resilience and better recovery.

Social buffering is a well-documented phenomenon in which the magnitude of an individual's stress response is reduced by the presence of an affiliative organism during stress exposure (9). This broadly applies to groups of mammals who have evolved to develop cooperative relationships regardless of genetic or familial bonds (9–11). In one study, triads of adult guinea pigs were housed together for long enough to develop affiliative bonds. When exposed to unfamiliar environments, participants in the original triad had reduced cortisol relative to isolated controls (12). Similarly, partnered rats displayed a reduction in stress-induced hyperthermia (13), and infants paired with mothers showed an abated response to threatening odors (14). Across species, social buffering is crucial for environmental learning and contextualization. Various studies have consistently replicated the buffering effect in healthy human participants (15,16) across a variety of different trauma types (17). Regardless of trauma, social support predicts a reduction in fear

ISSN: 2451-9022

expression (6,18,19). It has been suggested that over longer time scales, social relationships adaptively reduce fear conditioning and expression (20). However, there remains a need for more longitudinal study of posttrauma social support (21).

The neural mechanisms of the social buffering phenomenon are seemingly driven by the amygdala, which allows an individual to identify threats and respond appropriately (22–24). In young pups, maternal presence predicted dampened amygdala activity and increased avoidance of aversive stimuli (25). Several neuroimaging studies have investigated these effects in humans using social support cues (such as images of caregivers, romantic partners) in the context of threat tasks. These have implicated the ventromedial prefrontal cortex (vmPFC) and its connectivity with the amygdala in the observed buffering effects (26–29). We seek to extend this work to the context of threat processing following real-world traumatic events. Importantly, these could uncover brain regions or pathways that are involved in PTSD pathophysiology but also sensitive to psychosocial effects.

We investigated the neural correlates of social support and its relationship with later symptom trajectories in the AURORA (Advancing Understanding of Recovery After Trauma) study, a longitudinal, multisite study that encompasses the behavioral, cognitive, and affective facets of the posttraumatic experience (30). We explored longitudinal changes in PTSD symptoms as a function of individual differences in early posttrauma social support. We hypothesized a relationship between early posttrauma social support and decreased amygdala reactivity and increased vmPFC responsivity to social threat cues, a pattern that is typically seen in resilient individuals who experience trauma but do not have high PTSD symptoms (31–33). Moreover, we hypothesized greater white matter microstructural integrity in connections between the amygdala and vmPFC, such as the uncinate fasciculus (UF) and cingulum bundle, in participants who reported higher social support. Similar findings have been observed in trauma-exposed participants who did not develop PTSD (34–38).

METHODS AND MATERIALS

Participants

Participants were recruited at various emergency departments in the United States as part of the AURORA study (30). Inclusion criteria included traumatic events such as physical assault, sexual assault, falls >10 feet, and motor vehicle collision (MVC) (Table 1). Alternatively, traumatic events were qualifying if 1) individuals reported direct exposure or being witness to traumatic events that involved serious injury, violence, or death and 2) exposure was validated by research assistants. Exclusion criteria included administration of general anesthesia, long bone fractures, hemorrhagic injury, solid organ injury, not alert or oriented during enrollment, poor fluency in written or spoken English, visual and/or auditory impairment, self-inflicted or occupational injury, imprisonment, pregnancy, active breastfeeding, individuals confirming ongoing domestic violence, or active opioid use (i.e., morphine >20 mg or equivalent per day).

Overall, data were collected from 2626 individuals from the beginning of the study through July 2020 and released to investigators in the AURORA Freeze 3 data release. Individuals who resided near an AURORA deep phenotyping site were asked to participate in additional testing. A total of 436 individuals participated in focused neuroimaging assessments during deep phenotyping 2 weeks posttrauma. Of these, 369 completed functional magnetic resonance imaging (fMRI) and were considered for analysis in the current study. After quality control (detailed in the Supplement), data were excluded for head motion (n = 24), anatomical abnormalities (n = 7), technical reasons (n = 11), and lost stimulus timing data (n = 12 fMRI). This resulted in a final sample of 315 for analysis. Demographic characteristics of the final sample are reported in Table 1.

Of this final sample, 23 participants were excluded from diffusion MRI analysis due to head motion (n = 6), anatomical abnormalities (n = 11), and for technical reasons (n = 8). Two-week Patient-Reported Outcomes Measurement Information System (PROMIS) emotional support data were missing for 37, and 6-month PTSD Checklist for DSM-5 (PCL-5) data were missing for 88 individuals.

Table 1. Demographic and Clinical Features of the Sample, n = 315

Variable	n (%) or Mean (SD)
Sex/Gender	
Female	200 (63%)
Male	115 (37%)
Age, Years	33.63 (12.44)
Race/Ethnicity	
Black American	143 (46%)
Hispanic/Latin American	54 (17%)
Other American	13 (4%)
White American	104 (33%)
Employment	
Employed	199 (63%)
Retired	6 (2%)
Homemaker	10 (3%)
Student	10 (3%)
Unemployed, disabled, or other	52 (17%)
No response	38 (12%)
Total Family Income	
≤$19,000	73 (23%)
$19,001–$35,000	91 (29%)
$35,001–$50,000	43 (14%)
$50,001–$75,000	27 (9%)
$75,001–$100,000	19 (6%)
>$100,000	22 (7%)
No response	40 (12%)
Trauma Type	
Motor vehicle collision	226 (72%)
Physical assault	35 (11%)
Sexual assault	3 (0.9%)
Fall	19 (6%)
Mass trauma incident	1 (0.3%)
Nonmotorized collision	11 (3.5%)
Poisoning	0 (0%)
Burns	1 (0.3%)
Animal-related	9 (2.8%)
Other	10 (3.2%)

Assessments

Survey-based assessments were collected at week 2, week 8, month 3, and month 6 time points posttrauma. Symptoms were evaluated using the PCL-5, a 20-item self-report questionnaire rating the severity of posttrauma stress symptoms from 0 (not at all) to 4 (extremely) (39). PTSD symptom severity at the 6-month posttrauma time point was the primary outcome variable because reduced improvement of symptom severity within 3 to 6 months posttrauma confers a poorer long-term prognosis (40).

To quantify social support, participants completed an abbreviated version of the PROMIS Emotional Support Short Form 4a (41). The National Institute of Health's PROMIS measures contain a wide variety of self-reported outcome measures, and the emotional support questions show excellent reliability (Cronbach's α = 0.97) (42). The AURORA study included 3 questions from the original 4-item scale. Participants reported how often in the past 30 days (or 2 weeks for the 2-week posttrauma time point) that people in their personal life listened to them when they needed to talk, made them feel appreciated, or talked with them on a bad day. Answers ranged from 1 (never) to 5 (very often). The 3 items were summed to form an emotional support score with a range of 3 to 15. This modified version has also shown robust internal reliability (Cronbach's 2-week α = 0.88, Cronbach's 6-month α = 0.92). Additional information on participant demographics (such as sex/gender assigned at birth, ethnicity/racial identity, and traumatic event type and severity) were collected (outlined in Table 1). Trauma severity was assessed by participants' self-reported subjective perception of fatality regarding their traumatic event. This was scaled from 1 to 10, with 0 corresponding with "life was not threatened at all" and 10 with "came close to being killed or easily could have been killed."

Neuroimaging Acquisition

Images were collected at 5 sites, each of which used a 3T Siemens scanner. Acquisition parameters are listed by site in Table 2. fMRI was completed using blood oxygen level–dependent during cognitive tasks (task-based fMRI). Identical blood oxygen level–dependent fMRI scan parameters were used for acquisition of both resting-state and task data, although the time for each scan varied (see Table 1). Stimuli were presented using E-Prime 2.0 software (Psychology Software Tools). The neural processing of social threat cues was assessed using a fearful faces task. This task has been used in several studies of PTSD and has consistently demonstrated greater activation of the amygdala to fearful than to neutral faces (32,43–45). Blocks of fearful and neutral stimuli were sequentially presented, with the order of fearful and neutral blocks being counterbalanced across participants (15 blocks each). In each block, 8 faces (4 male, 4 female) were presented for 500 ms each, with a 500-ms fixation cross presented after each face. Every 10th block, participants received a 10,000-ms fixation cross as a "rest period" and were instructed to "relax and look at the screen." Diffusion-weighted imaging was completed to assess microstructural properties of brain white matter, which has previously been associated with several posttraumatic outcomes. For each participant, a 64-direction diffusion-weighted imaging sequence was used with a 2-mm isotropic resolution (but see Table 2 to note one

Table 2. Neuroimaging Site Parameters

Modality	Site 1, Siemens MAGNETOM 3T TIM Trio, 12-Channel Head Coil	Site 2, Siemens MAGNETOM 3T TIM Trio, 12-Channel Head Coil	Site 3, Siemens MAGNETOM 3T Verio, 12-Channel Head Coil	Site 4, Siemens MAGNETOM 3T Prisma, 20-Channel Head Coil	Site 5, Siemens MAGNETOM 3T Prisma, 32-Channel Head Coil
T1-Weighted	TR = 2530 ms, TEs = 1.74/3.6/5.46/7.32 ms, TI = 1260 ms, flip angle = 7°, FOV = 256 mm, slices = 176, voxel size = 1 × 1 × 1 mm	TR = 2530 ms, TEs = 1.74/3.6/5.46/7.32 ms, TI = 1260 ms, flip angle = 7°, FOV = 256 mm, slices = 176, voxel size = 1 × 1 × 1 mm	TR = 2530 ms, TEs = 1.79/3.65/5.51/7.37 ms, TI = 1260 ms, flip angle = 7°, FOV = 256 mm, slices = 176, voxel size = 1 × 1 × 1 mm	TR = 2300 ms, TE = 2.96 ms, TI = 900 ms, flip angle = 9°, FOV = 256 mm, slices = 176, voxel size = 1.2 × 1.0 × 1.0 mm	TR = 2530 ms, TEs = 2.24/4.1/5.96/7.82 ms, TI = 1350 ms, flip angle = 7°, FOV = 256 mm, slices = 176, voxel size = 1 × 1 × 1 mm
Functional MRI	TR = 2360 ms, TE = 30 ms, flip angle = 70°, FOV = 210 mm, slices = 44, voxel size = 3 × 2.72 × 2.72 mm, 0.5-mm gap	TR = 2360 ms, TE = 30 ms, flip angle = 70°, FOV = 210 mm, slices = 44, voxel size = 3 × 3 × 3 mm, 0.5-mm gap	TR = 2360 ms, TE = 30 ms, flip angle = 70°, FOV = 210 mm, slices = 42, voxel size = 3 × 2.72 × 2.72 mm, 0.5-mm gap	TR = 2360 ms, TE = 29 ms, flip angle = 70°, FOV = 210 mm, slices = 44, voxel size = 3 × 2.72 × 2.72 mm, 0.5-mm gap	TR = 2360 ms, TE = 29 ms, flip angle = 90°, FOV = 210 mm, slices = 44, voxel size = 3 × 2.72 × 2.72 mm, 0.5-mm gap
Diffusion MRI	TR = 7700 ms, TE = 85 ms, FOV = 212 mm, flip angle = 90°, voxel size = 2 × 2 × 2 mm, *b*-value = 1000 s/mm^2, 64 directions, 7 b0 images	TR = 7700 ms, TE = 85 ms, FOV = 212 mm, flip angle = 90°, voxel size = 2 × 2 × 2 mm, *b*-value = 1000 s/mm^2, 64 directions, 7 b0 images	TR = 12,000 ms, TE = 85 ms, FOV = 212 mm, flip angle = 90°, voxel size = 2 × 2 × 2 mm, *b*-value = 1000 s/mm^2, 64 directions, 7 b0 images	TR = 7000 ms, TE = 74 ms, FOV = 212 mm, flip angle = 90°, voxel size = 2 × 1.8 × 1.8 mm, *b*-value = 1000 s/mm^2, 64 directions, 7 b0 images	TR = 7700 ms, TE = 67 ms, FOV = 212 mm, flip angle = 90°, voxel size = 2 × 2 × 2 mm, *b*-value = 1000 s/mm^2, 64 directions, 7 b0 images

FOV, field of view; MRI, magnetic resonance imaging; TE, echo time; TI, inversion time; TR, repetition time.

site with nonisotropic dimensions), and diffusion-weighted images were collected at b = 1000. In addition, 7 non-weighted diffusion images were collected.

Neuroimaging Data Analysis

Quality control and preprocessing steps are elaborated on in the Supplement. We conducted a first-level general linear model analysis fitted for individual participants' neuroimaging data. The fearful faces task was modeled as an 8-second block of either fearful or neutral stimuli, convolved with the canonical hemodynamic response curve. Mean contrast values were extracted for the comparison of fearful versus neutral conditions from regions of interest (ROIs) reflecting anatomical boundaries of regions previously implicated in emotional arousal and PTSD (31,33,46–49). These included the left and right amygdala (CIT168 atlas), left and right hippocampus (Hammers atlas), left and right insula (Harvard/Oxford cortical atlas), and bilateral Brodmann areas 32 (dorsal anterior cingulate cortex [ACC]) and 25 (subgenual ACC) (WFU PickAtlas) (50–53). To explore regions outside of the a priori ROIs, we employed a voxelwise, whole-brain, random-effects analysis with a term for 2-week emotional support, as well as covarying for site of neuroimaging data collection. A second whole-brain model assessed the association with 6-month PTSD symptom scores while covarying for site of neuroimaging data collection. Whole-brain statistical thresholds were established using the built-in SPM cluster correction feature to account for multiple comparisons (54), following random field theory (55,56). A cluster size threshold of 346 voxels was needed to reach a familywise error–corrected $p < .05$ under an initial cluster-forming threshold of $p < .005$. Mean contrast estimates for threat reactivity (fearful > neutral) within significant clusters were extracted using the REX (ROI extraction) toolbox (57) for visualization and follow-up testing.

Diffusion-weighted imaging data were processed similarly to previous methods to remove artifacts and maintain data quality. A substantial body of evidence has shown over-reactivity of the amygdala in PTSD and other comorbid disorders (58), directing our focus to tracts with relevant ties to this region. We used tract-based spatial statistics to extract the mean fractional anisotropy (FA) value for the bilateral (mean of left and right) cingulate part of the cingulum bundle (CGC), bilateral hippocampal part of the cingulum bundle, and bilateral UF (59,60).

Statistical Analyses

Statistical analyses were run on R version 4.2.0 and RStudio software platforms. All primary hypothesis-testing models controlled for participant sex/gender (designated on birth certificate) and self-reported ethnic/racial identity, age, and trauma severity. A strong body of evidence demonstrates that sex/gender and racial/ethnic identity are contributing factors to worse PTSD outcomes (61–64). All models were then repeated without these covariates to provide a reference comparison and minimize potential confounding effects of these variables. Neuroimaging models also included a covariate for the site of data collection.

To investigate the relationship between social buffering and PTSD symptoms, we used a linear regression model assessing the effect of 2-week PROMIS emotional support scores on PCL-5 scores at the 6-month time point. Follow-up testing assessed whether there was also an effect of 2-week emotional support on concurrent PTSD symptoms. Subgroup analyses stratifying MVC and non-MVC trauma types were conducted to provide additional context (Table S1A, B).

Then, we investigated areas of the brain that may be preferentially engaged in processing social threat cues and are also receptive to emotional support. We hypothesized that participants who reported higher levels of early posttrauma emotional support would demonstrate reduced activation of brain regions that support emotional arousal responses. To test this, we conducted regression models assessing the effects of 2-week emotional support on reactivity to fearful faces within the amygdala, hippocampus, insula, dorsal ACC, and subgenual ACC ROIs, with correction for multiple comparisons using the Benjamini-Hochberg false discovery rate (FDR). For brain regions that exhibited a significant association with early emotional support, we conducted planned follow-up analyses to explore their relationship with 6-month PTSD symptoms.

Then, we tested the hypothesis that early emotional support would be positively related to FA of the UF, CGC, and bilateral hippocampal part of the cingulum bundle. Linear regression models evaluated the relationship between 2-week emotional support and FA values in tracts of interest. Additional analyses were then used to examine the impact of 6-month PTSD symptom severity on tracts that exhibited a significant association with early emotional support. Multiple comparisons were corrected using the Benjamini-Hochberg FDR.

Finally, mediation analyses were used to characterize whether brain ROIs/tracts of interest mediated the effects of 2-week social support on 6-month PTSD symptoms.

RESULTS

Greater early posttrauma emotional support predicted lower PTSD symptoms at the 6-month time point (Figure 1 and Table 3). The effect size was similar but not significant in a model without covariates ($\beta_{208} = -0.120$, $p = .061$). Emotional

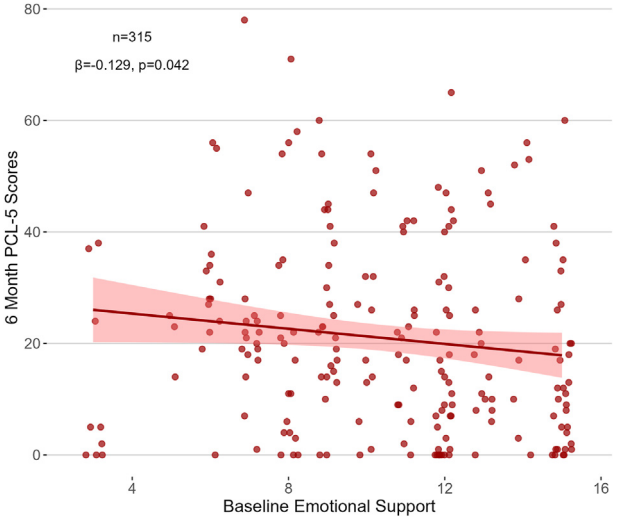

Figure 1. Scatterplot demonstrating negative correlation between early emotional support and 6-month posttraumatic stress disorder symptoms. PCL-5, PTSD Checklist for DSM-5.

Table 3. Effect of 2-Week Emotional Support on 6-Month Posttraumatic Stress Disorder Symptom Severity

	β	SE	*t*	*p*
2-Week PROMIS Scores	−0.129	0.063	−2.040	.042
Sex/Gender	0.137	0.066	2.079	.039
Ethnic/Racial Identity	−0.047	0.070	−0.673	.502
Trauma Severity	0.050	0.065	0.769	.443
Age	0.123	0.064	1.922	.056

PROMIS, Patient-Reported Outcomes Measurement Information System.

support scores also demonstrated a negative association with 2-week PTSD symptoms ($\beta_{261} = -0.155$, $p = .008$). Analyses stratified by trauma type showed the buffering effect for MVCs ($n = 197$), but not for the other trauma types ($n = 80$) (Table S1A, B).

Effect of Emotional Support on fMRI Reactivity to Social Threat Cues

Then, we evaluated the association between early posttrauma emotional support and neural responses to social threat cues. In the total sample, the task engaged significant bilateral amygdala responses to fearful > neutral faces (familywise error–corrected $p < .05$) (Figure S1). However, there were no significant associations between emotional support and activation in any of the ROIs, $p_{FDR} > .05$, in models conducted with or without covariates (Table S2A, B). Whole-brain analyses showed a positive correlation between early posttrauma emotional support and the response to fearful > neutral face stimuli in a large cluster within the bilateral posterior cingulate cortex (PCC) (x, y, z = −4, −32, 34, $Z = 3.88$, $k = 346$) (Figure 2). Then, we extracted the fearful > neutral contrast estimate from this cluster to test whether PCC activation was also related to risk for later PTSD symptoms. However, PCC activation was not associated with 6-month PCL-5 scores ($\beta_{208} = 1.465$, $p = .743$).

Effect of Emotional Support on White Matter Microstructural Integrity in Threat-Relevant Tracts

Effects of 2-week emotional support on diffusion MRI tracts of interest are reported in Table 4 (with covariates) and Table S3 (without covariates). Emotional support was positively correlated with FA of the CGC (Figure 3) and UF, but not the bilateral hippocampal part of the cingulum bundle. CGC FA was also negatively associated with later PTSD symptom severity at 6 months posttrauma ($\beta_{207} = -0.149$, $p = .027$), whereas UF FA was not ($\beta_{207} = -0.038$, $p = .587$). Mediation analysis with CGC FA showed a reduction in the effect of early posttrauma emotional support on later PTSD symptom severity (Figure 4), but the magnitude of the mediation effect was not statistically significant (Sobel $Z = -1.452$, $p = .146$).

DISCUSSION

In the current study, we examined relationships between social support and longitudinal posttraumatic stress. Our findings are consistent with those of previous studies that demonstrated that early posttrauma support significantly mitigated long-term PTSD severity. When we stratified our models by trauma type, we found that this effect was present only in our MVC trauma group, which comprises much of our study population. This was not observed in the non-MVC group, suggesting that additional studies of social support focusing on other trauma types are necessary to improve the generalizability of this effect. The neuroimaging findings did not fully support the hypothesis that social support would influence the amygdala, vmPFC, and white matter pathways between these regions. Instead, early posttrauma social support was linked to a greater PCC response to social threat cues and greater FA (associated with white matter microstructural integrity) in both the UF and CGC, with the latter showing effects on later PTSD symptom severity. Together, the findings suggest that mechanisms of social buffering effects on PTSD symptoms may be more complex than was previously understood.

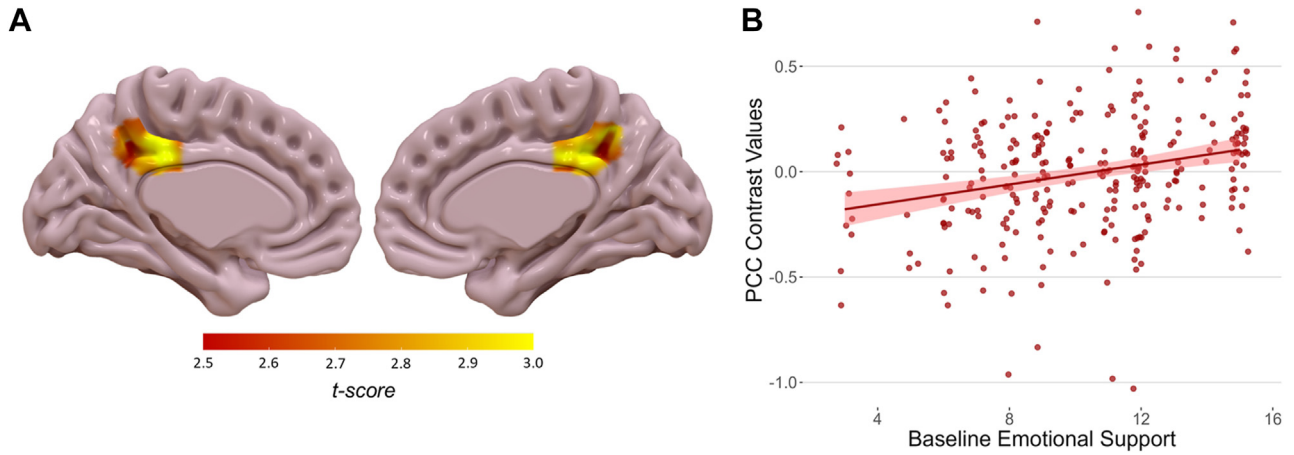

Figure 2. **(A)** Midsagittal brain reconstruction showing bilateral activation of posterior cingulate cortex (PCC) in conjunction with early 2-week emotional support (highlighted and gradated with heat map overlay). **(B)** Correlation plot between average contrast values for the PCC cluster as a function of 2-week emotional support scores. The trend line demonstrates a positive association between PCC and 2-week Patient-Reported Outcomes Measurement Information System (PROMIS) scores.

Table 4. Effect of 2-Week Emotional Support on A Priori White Matter Tracts[a]

	β	SE	*t*	*p*	p_{FDR}
Bilateral Cingulum—Cingulate Gyrus	0.156	0.060	2.587	.010	.010
Bilateral Cingulum—Hippocampus	−0.014	0.062	−0.231	.817	.817
Bilateral Uncinate Fasciculus	0.159	0.061	2.601	.010	.010

FDR, false discovery rate.

[a]Covariates included sex/gender, ethnic/racial identity, trauma severity, age, and neuroimaging site.

Early and sustained support is critical throughout the duration of trauma recovery, with some studies showing potential positive physiological impacts in patients who are recovering from chronic disease and major trauma (65–68). Many studies of social buffering have focused on the reduction of activity within the hypothalamic-pituitary-adrenal axis and have specifically shown lower glucocorticoid levels in response to a variety of stressors (15,69,70). Conversely, the absence of psychosocial support has been shown to indicate abnormal emotion regulation, thereby increasing risk for worse mental health outcomes (18,71–73).

The interplay between fear regulation, memory, and emotion processing is key to understanding trauma resilience (74,75). Threat processing clearly depends on synaptic connections between the PFC and amygdala (23,24). Seemingly, the ventromedial portion targets the central nucleus of the amygdala to inhibit fear, and the dorsomedial region synapses on the basolateral amygdala to promote fear. Thus, prefrontal inputs to the amygdala theoretically allow for sensitivity to emotional support and the social buffering phenomenon (76,77). However, in our analyses, we did not find any changes in activity within the amygdala or evidence suggesting that social support improved engagement of prefrontal regions. However, this is not entirely unexpected. The experimental paradigm of social buffering in previous literature reflects an extremely controlled application of stress to a participant in the presence of a conspecific. It may be that different brain regions mediate the social buffering effect in humans versus rodents or alternatively that there are different regions involved for controlled laboratory stressors versus real-world traumatic events. Human studies have shown that having a conspecific present while being presented with threat cues and imaged in a controlled environment was associated with dampened activity in the amygdala, along with various other cortical regions (77–79). With our study, we aimed to expand on this literature by analyzing real-world traumatic events rather than laboratory stress or threat paradigms and observing the dynamics of stress on a longer longitudinal scale than earlier models. The fact that we did not observe effects on amygdala reactivity to threat suggests that canonical threat regulation circuitry may be impacted most strongly by direct social influences such as the presence of a close other during a laboratory stress task and may be less relevant to the persistent effects of social support in the context of real-world traumatic stress. More exploration is needed to understand the time frame with which social support may influence threat processing and amygdala reactivity.

We did find a positive association between early posttrauma social support and FA in the UF at 2 weeks posttrauma, and this association remained significant after FDR correction. This tract ipsilaterally bridges the orbitofrontal cortex and vmPFC with the anterior temporal lobes and amygdala (80). Degradation of this tract has been implicated in abnormal emotion regulation (81), which when combined with deficiencies in episodic memory contextualization (82,83), may lead to improper behavioral responses to benign environmental stimuli. Although we did not find an association between the UF and later PTSD symptom severity, dysfunctional connectivity within the UF has been shown to predict reduced regulation of amygdala reactivity by the vmPFC and higher risk for chronic PTSD (34,36,84,85). Whether the robust social support provided before trauma as opposed to early after trauma affected UF integrity remains to be seen, because the current study did not include the pretrauma neuroimaging that would be necessary to distinguish between these two possibilities. However, given that FA is likely to be relatively stable across the short time frame of 2 weeks between trauma exposure and our neuroimaging observations, we speculate that the FA

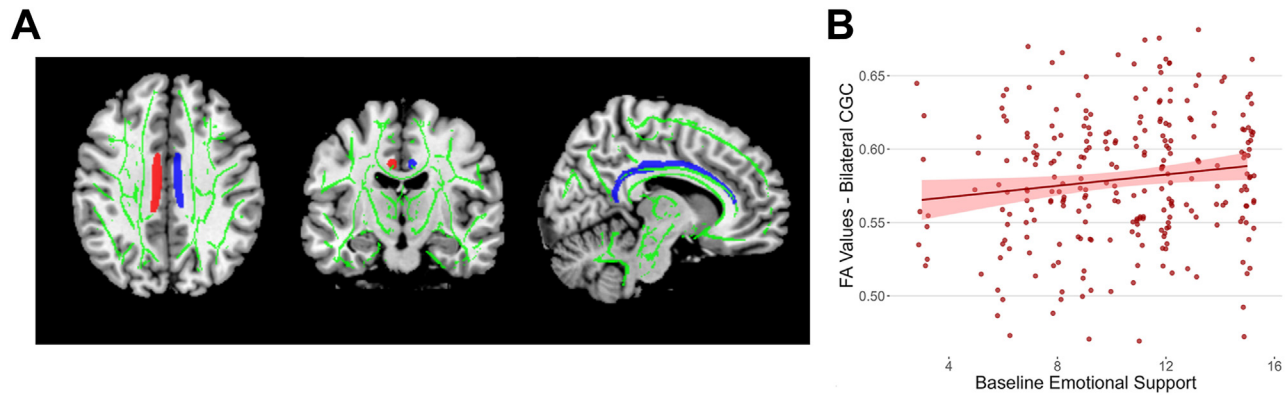

Figure 3. **(A)** Visual schematic highlighting the bilateral cingulum (regions highlighted in red and blue, overlaid on ENIGMA [Enhancing Neuro Imaging Genetics through Meta Analysis] diffusion tensor imaging skeleton in green). **(B)** Plot showing positive correlation between diffusion tensor imaging values and early emotional support scores. CGC, cingulate part of the cingulum bundle; FA, fractional anisotropy.

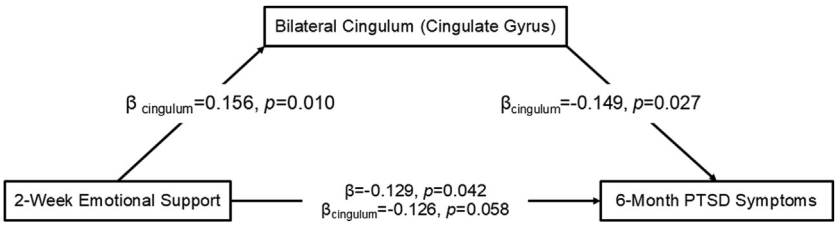

Figure 4. Statistical summary of effect of bilateral cingulum on longitudinal posttraumatic stress disorder (PTSD) scores as a function of early 2-week emotional support.

findings likely reflect pretrauma protective effects of high social support and corresponding high FA of the UF.

In whole-brain fMRI analyses, we recorded significant positive correlations between early posttrauma social support and engagement of the PCC to threat cues. Our findings suggest a complex relationship between threat processing and the default mode network (DMN) (86). The PCC serves as the posterior hub of the DMN, which is responsible for internal and self-referential cognition (87,88) and modulating behavioral responses to various stressful situations (89). Numerous imaging studies with patients with PTSD have shown disrupted connectivity of the PCC with the frontal gyrus, subgenual ACC, and thalamus, among others (90–93). The DMN generally shows reduced connectivity in PTSD but has spared connections in posterior regions of the network (91,94,95). While some neuroimaging PTSD studies have highlighted a reduction in activity within the posteromedial area of the parietal lobe (96), Sippel *et al.* (97) recently observed hyperactivity in this region in individuals with PTSD who had poor social networks. Posterior DMN connectivity may contribute to altered social cognition in individuals at risk for PTSD. Several recent studies of social buffering effects in healthy adults point to an extended network of regions whose functioning mediates buffering effects, with notable buffering effects on the response to threat cues in the PCC and precuneus (98–100). This raises the possibility that the PCC, and the posterior DMN more broadly, may be critical facilitators of social buffering effects. This may be most apparent either in the context of trauma recovery or potentially in adults given that much of the social buffering literature points to primary effects within the amygdala during childhood. For example, buffering effects of parental cues on the amygdala response are most pronounced before age 10 and are less apparent by the transition to adolescence (100). It may be that adults with more robust social support can engage regions of the DMN to better contextualize social threat cues and provide an adequately measured stress response.

While we did not observe a significant mediating effect of the CGC on PTSD symptoms, this tract was positively correlated with early emotional support. The CGC connects the posterior (PCC/precuneus) and anterior (medial prefrontal) components of the DMN (101–104). Patients with PTSD demonstrate reduced FA of the cingulum bundle with greater PTSD symptom severity (38,102,105–107). Perhaps individuals with high social support engage the PCC in response to threat cues, and signals are conducted through white matter tract connections in the cingulum bundle. This may lead to altered communication with the anterior prefrontal DMN and additional downstream regions, which remains to be explored in the future.

Following Hornstein and Eisenberger's theoretical model of social cues as "prepared safety stimuli" (27), we conjecture that social support cues actively inhibit conditioned fear, including learned responses to trauma reminders in the case of real-world traumatic stress. One potential neurobiological mechanism may be through a release of oxytocin stimulated by social support cues, which contribute to a reduction of anxiety in stressful situations (15). Preliminary studies have demonstrated the role of oxytocin in modulating social networks including the dorsal DMN and inhibiting stress responses in the amygdala and ACC (108). Alternatively, social buffering has been shown to dampen hypothalamic-pituitary-adrenal axis activity with a direct reduction of cortisol release and correlation with lower levels of proinflammatory cytokines (11,15,109,110).

Limitations

Key aspects of this study put limits on its interpretation and generalizability. Notably, the measure of social support was limited by the brief self-report measures used in the AURORA study. The complexity of social networks and varied forms of social support were not fully quantified here. To maximize the generalizability of future studies, qualitative measures should account for aspects of support that may vary based on socioeconomic, cultural, physical, and other needs. Furthermore, it is important to consider how different phenotypes of PTSD respond to social support–focused interventions. Perhaps PTSD with primary disruptions in social cognition (criteria D) or arousal (criteria E) will prove to be more sensitive to social buffering.

Conclusions and Future Directions

Importantly, our results suggest that early posttrauma social support has benefits for the longitudinal reduction of self-reported PTSD symptoms. However, the consistency of emotional support throughout recovery may prove more important for patient outcomes than the magnitude of support at the time of trauma. Additionally, future work should consider a more reciprocal relationship in which the evolution of PTSD symptoms may increase social isolation or encourage strengthened supportive networks.

Future neuroimaging research in this field should probe working mechanisms on higher-resolution, temporal changes posttrauma, from cortical activity to white matter tract microstructure. It would also be interesting to observe outcomes in randomized trials where positive social behaviors are recommended in a managed plan for posttrauma recovery, including the PCC as a hypothesized target and mediator of treatment effects. This would augment the functional characterization of

these regions, but more importantly, it would provide the field with a novel foundation to refine the definition of posttraumatic stress as being dependent on the social context.

ACKNOWLEDGMENTS AND DISCLOSURES

This work was supported by the National Institute of Mental Health (Grant No. U01MH110925 [to SAM]), the U.S. Army MRMC (to SAM), One Mind (to SAM), and The Mayday Fund (to SAM). The content is solely the responsibility of the authors and does not necessarily represent the official views of any of the funders.

Data and/or research tools used in the preparation of this manuscript were obtained from the NIMH Data Archive (NDA). NDA is a collaborative informatics system created by the National Institutes of Health to provide a national resource to support and accelerate research in mental health. Dataset identifier(s): https://nda.nih.gov/study.html?id=2640. This article reflects the views of the authors and may not reflect the opinions or views of the NIH or of the submitters submitting original data to NDA.

JLCS and JSS were responsible for the design and conceptualization of the study. JSS was responsible for data collection and recruitment. JLCS and JSS were responsible for data processing and statistical analyses and initial drafting of the article. All authors revised the manuscript critically for important intellectual context and agree to be accountable for all aspects of the work and ensure the accuracy and integrity of the findings.

We thank the trauma survivors participating in the AURORA study. Their time and effort during a challenging period of their lives make our efforts to improve recovery for future trauma survivors possible.

NGH reports support from NIMH (Grant No. K01MH129828) and from the Brain & Behavior Research Foundation. SJHvR is supported by NIMH (Grant No. K01MH121653). TJ receives support from NIMH (Grant No. R01 MH129495). TCN has received research support from the National Institutes of Health, the Veterans Administration, and Rainwater Charitable Foundation and consulting income from Jazz Pharmaceuticals. LTG receives support from NIMH (Grant No. R01 MH121617) and is on the board of the Many Brains Project. Her family also has equity in Intelerad Medical Systems, Inc. SLR reported serving as secretary of the Society of Biological Psychiatry; serving as a board member of Community Psychiatry and Mindpath Health; serving as a board member of National Association of Behavioral Healthcare; serving as secretary and a board member for the Anxiety and Depression Association of America; serving as a board member of the National Network of Depression Centers; receiving royalties from Oxford University Press, American Psychiatric Publishing Inc., and Springer Publishing; and receiving personal fees from the Society of Biological Psychiatry, Community Psychiatry and Mindpath Health, and National Association of Behavioral Healthcare outside the submitted work. CWJ has no competing interests related to this work, although he has been an investigator on studies funded by AstraZeneca, Vapotherm, Abbott, and Ophirex. Over the past 3 years, DAPi has received consulting fees from Boehringer Ingelheim, Compass Pathways, Engrail Therapeutics, Neumora Therapeutics (formerly BlackThorn Therapeutics), Neurocrine Biosciences, Neuroscience Software, Otsuka Pharmaceuticals, Sage Therapeutics, Sama Therapeutics, and Takeda Pharmaceuticals; honoraria from the American Psychological Association, Psychonomic Society, and Springer (for editorial work) and Alkermes; and research funding from the Bird Foundation, Brain & Behavior Research Foundation, the Defense Advanced Research Projects Agency, Millennium Pharmaceuticals, and the NIMH. In addition, he has received stock options from Compass Pathways, Engrail Therapeutics, Neumora Therapeutics (former BlackThorn Therapeutics), and Neuroscience Software. SEH has no competing interest related to this work, although in the last 3 years he has received research funding from Aptinyx and Arbor Medical Innovations and consulting payments from Memorial Sloan Kettering Cancer Center, Wayne State University, Indiana University Indianapolis, the Ohio State University, Dana Farber Cancer Institute, and Stanford University. KJR has performed scientific consultation for BioXcel, Bionomics, Acer, and Jazz Pharma; serves on Scientific Advisory Boards for Sage, Boehringer Ingelheim, Senseye, and the Brain Research Foundation; and has received sponsored research support from Alto Neuroscience. KCK has been a paid scientific consultant for the U.S. Department of Justice and Covington Burling, LLP over the last 3 years. She receives royalties from Guilford Press and Oxford University Press. SAM has served as a consultant for Walter Reed Army Institute for Research, Arbor Medical Innovations, and BioXcel Therapeutics, Inc. All other authors report no biomedical financial interests or potential conflicts of interest.

ARTICLE INFORMATION

From the Department of Psychiatry and Behavioral Sciences, Emory University School of Medicine, Atlanta, Georgia (JLCS); Division of Depression and Anxiety, McLean Hospital, Belmont, Massachusetts (NGH, LAML, DAPi, KJR); Department of Psychiatry, Harvard Medical School, Boston, Massachusetts (NGH, LAML, LTG, SLR, DAPi, KJR); Department of Psychiatry and Behavioral Sciences, Emory University School of Medicine, Atlanta, Georgia (SJHvR, TDE, JSS); Department of Psychiatry and Behavioral Neurosciences, Wayne State University, Detroit, Michigan (TJ); Department of Epidemiology, Brown University, Providence, Rhode Island (FLB); Department of Emergency Medicine, Brown University, Providence, Rhode Island (FLB); Institute for Trauma Recovery, Department of Anesthesiology, University of North Carolina at Chapel Hill, Chapel Hill, North Carolina (XA, SDL); Department of Psychiatry and Department of Neurology, University of California San Francisco, San Francisco, California (TCN); Institute for Technology in Psychiatry, McLean Hospital, Belmont, Massachusetts (LTG, SLR); The Many Brains Project, Belmont, Massachusetts (LTG); Department of Psychology and Neuroscience and Department of Sociology, University of North Carolina at Chapel Hill, Chapel Hill, North Carolina (KAB); Department of Psychiatry, McLean Hospital, Belmont, Massachusetts (SLR); Department of Emergency Medicine, University of Massachusetts Chan Medical School, Worcester, Massachusetts (JPH); Department of Emergency Medicine, Vanderbilt University Medical Center, Nashville, Tennessee (ABS); Department of Emergency Medicine, Henry Ford Health System, Detroit, Michigan (CL); Department of Emergency Medicine, Indiana University School of Medicine, Indianapolis, Indiana (PIM); Department of Emergency Medicine, University of Florida College of Medicine, Jacksonville, Jacksonville, Florida (PLH, SS); Department of Emergency Medicine, Cooper Medical School of Rowan University, Camden, New Jersey (CWJ); Department of Emergency Medicine, Ohio State University College of Medicine, Columbus, Ohio (BEP); Ohio State University College of Nursing, Columbus, Ohio (BEP); Department of Surgery and Department of Neurosurgery, University of Pennsylvania, Philadelphia, Pennsylvania (JLP); Perelman School of Medicine, University of Pennsylvania, Philadelphia, Pennsylvania (JLP, MJS); Division of Traumatology, Surgical Critical Care and Emergency Surgery, Department of Surgery, University of Pennsylvania, Philadelphia, Pennsylvania (MJS); Department of Emergency Medicine, Einstein Medical Center, Philadelphia, Pennsylvania (EH); Department of Emergency Medicine, Wayne State University, Ascension St. John Hospital, Detroit, Michigan (CP); Department of Emergency Medicine, Massachusetts General Hospital, Boston, Massachusetts (DAPe); Department of Emergency Medicine, Brigham and Women's Hospital, Boston, Massachusetts (RCM, LDS); Department of Emergency Medicine, Trinity Health, Ann Arbor, Ypsilanti, Michigan (RMD); Department of Emergency Medicine, University of Massachusetts Medical School-Baystate, Springfield, Massachusetts (NKR); Department of Emergency Medicine, Wayne State University, Detroit Receiving Hospital, Detroit, Michigan (BJO); Department of Emergency Medicine, McGovern Medical School at UTHealth, Houston, Texas (PS); Department of Emergency Medicine, Harvard Medical School, Boston, Massachusetts (LDS); Department of Psychological Sciences, University of Missouri – St. Louis, St. Louis, Missouri (SEB); Department of Anesthesiology, University of Michigan Medical School, Ann Arbor, Michigan (SEH); Department of Internal Medicine-Rheumatology, University of Michigan Medical School, Ann Arbor, Michigan (SEH); Department of Epidemiology, Harvard T.H. Chan School of Public Health, Harvard University, Boston, Massachusetts (KCK); Department of Emergency Medicine, University of North Carolina at Chapel Hill, Chapel Hill, North Carolina (SAM); and Institute for Trauma Recovery, Department of Psychiatry, University of North Carolina at Chapel Hill, Chapel Hill, North Carolina (SAM).

Address correspondence to Jennifer S. Stevens, Ph.D., at jennifer.stevens@emory.edu.

Received Jun 14, 2024; revised Nov 1, 2024; accepted Nov 6, 2024.

Supplementary material cited in this article is available online at https://doi.org/10.1016/j.bpsc.2024.11.011.

REFERENCES

1. Keane TM, Marshall AD, Taft CT (2006): Posttraumatic stress disorder: Etiology, epidemiology, and treatment outcome. Annu Rev Clin Psychol 2:161–197.
2. Yehuda R, Hoge CW, McFarlane AC, Vermetten E, Lanius RA, Nievergelt CM, *et al.* (2015): Post-traumatic stress disorder. Nat Rev Dis Primers 1:15057.
3. Brewin CR, Andrews B, Valentine JD (2000): Meta-analysis of risk factors for posttraumatic stress disorder in trauma-exposed adults. J Consult Clin Psychol 68:748–766.
4. DiGangi JA, Gomez D, Mendoza L, Jason LA, Keys CB, Koenen KC (2013): Pretrauma risk factors for posttraumatic stress disorder: A systematic review of the literature. Clin Psychol Rev 33:728–744.
5. Ozer EJ, Best SR, Lipsey TL, Weiss DS (2003): Predictors of posttraumatic stress disorder and symptoms in adults: A meta-analysis. Psychol Bull 129:52–73.
6. Dworkin ER, Ojalehto H, Bedard-Gilligan MA, Cadigan JM, Kaysen D (2018): Social support predicts reductions in PTSD symptoms when substances are not used to cope: A longitudinal study of sexual assault survivors. J Affect Disord 229:135–140.
7. Tirone V, Orlowska D, Lofgreen AM, Blais RK, Stevens NR, Klassen B, *et al.* (2021): The association between social support and posttraumatic stress symptoms among survivors of betrayal trauma: A meta-analysis. Eur J Psychotraumatol 12:1883925.
8. Panagioti M, Gooding PA, Taylor PJ, Tarrier N (2014): Perceived social support buffers the impact of PTSD symptoms on suicidal behavior: Implications into suicide resilience research. Compr Psychiatry 55:104–112.
9. Kiyokawa Y, Hennessy MB (2018): Comparative studies of social buffering: A consideration of approaches, terminology, and pitfalls. Neurosci Biobehav Rev 86:131–141.
10. Kikusui T, Winslow JT, Mori Y (2006): Social buffering: Relief from stress and anxiety. Philos Trans R Soc Lond B Biol Sci 361:2215–2228.
11. Hennessy MB, Kaiser S, Sachser N (2009): Social buffering of the stress response: Diversity, mechanisms, and functions. Front Neuroendocrinol 30:470–482.
12. Hennessy MB, Zate R, Maken DS (2008): Social buffering of the cortisol response of adult female guinea pigs. Physiol Behav 93:883–888.
13. Kiyokawa Y, Kikusui T, Takeuchi Y, Mori Y (2004): Partner's stress status influences social buffering effects in rats. Behav Neurosci 118:798–804.
14. Moriceau S, Sullivan RM (2006): Maternal presence serves as a switch between learning fear and attraction in infancy. Nat Neurosci 9:1004–1006.
15. Heinrichs M, Baumgartner T, Kirschbaum C, Ehlert U (2003): Social support and oxytocin interact to suppress cortisol and subjective responses to psychosocial stress. Biol Psychiatry 54:1389–1398.
16. Eisenberger NI, Taylor SE, Gable SL, Hilmert CJ, Lieberman MD (2007): Neural pathways link social support to attenuated neuroendocrine stress responses. Neuroimage 35:1601–1612.
17. Galea S, Ahern J, Resnick H, Kilpatrick D, Bucuvalas M, Gold J, Vlahov D (2002): Psychological sequelae of the September 11 terrorist attacks in New York City. N Engl J Med 346:982–987.
18. Zhao G, Xie F, Li S, Ding Y, Li X, Liu H (2022): The relationship between perceived social support with anxiety, depression, and insomnia among Chinese college students during the COVID-19 pandemic: The mediating role of self-control. Front Psychiatry 13:994376.
19. Kaniasty K, Norris FH (2008): Longitudinal linkages between perceived social support and posttraumatic stress symptoms: Sequential roles of social causation and social selection. J Trauma Stress 21:274–281.
20. Hornstein EA, Craske MG, Fanselow MS, Eisenberger NI (2022): Reclassifying the unique inhibitory properties of social support figures: A roadmap for exploring prepared fear suppression. Biol Psychiatry 91:778–785.
21. Wang Y, Chung MC, Wang N, Yu X, Kenardy J (2021): Social support and posttraumatic stress disorder: A meta-analysis of longitudinal studies. Clin Psychol Rev 85:101998.
22. Adolphs R (1999): Social cognition and the human brain. Trends Cogn Sci 3:469–479.
23. Adhikari A, Topiwala MA, Gordon JA (2010): Synchronized activity between the ventral hippocampus and the medial prefrontal cortex during anxiety. Neuron 65:257–269.
24. Hagihara KM, Bukalo O, Zeller M, Aksoy-Aksel A, Karalis N, Limoges A, *et al.* (2021): Intercalated amygdala clusters orchestrate a switch in fear state. Nature 594:403–407.
25. Sullivan RM, Holman PJ (2010): Transitions in sensitive period attachment learning in infancy: The role of corticosterone. Neurosci Biobehav Rev 34:835–844.
26. Gee DG, Gabard-Durnam L, Telzer EH, Humphreys KL, Goff B, Shapiro M, *et al.* (2014): Maternal buffering of human amygdala-prefrontal circuitry during childhood but not during adolescence. Psychol Sci 25:2067–2078.
27. Eisenberger NI, Master SL, Inagaki TK, Taylor SE, Shirinyan D, Lieberman MD, Naliboff BD (2011): Attachment figures activate a safety signal-related neural region and reduce pain experience. Proc Natl Acad Sci U S A 108:11721–11726.
28. Qi R, Luo Y, Zhang L, Weng Y, Surento W, Jahanshad N, *et al.* (2020): Social support modulates the association between PTSD diagnosis and medial frontal volume in Chinese adults who lost their only child. Neurobiol Stress 13:100227.
29. Sato W, Kochiyama T, Kubota Y, Uono S, Sawada R, Yoshimura S, Toichi M (2016): The association between perceived social support and amygdala structure. Neuropsychologia 85:237–244.
30. McLean SA, Ressler K, Koenen KC, Neylan T, Germine L, Jovanovic T, *et al.* (2020): The Aurora Study: A longitudinal, multimodal library of brain biology and function after traumatic stress exposure. Mol Psychiatry 25:283–296.
31. Shin LM, Rauch SL, Pitman RK (2006): Amygdala, medial prefrontal cortex, and hippocampal function in PTSD. Ann N Y Acad Sci 1071:67–79.
32. Stevens JS, Jovanovic T, Fani N, Ely TD, Glover EM, Bradley B, Ressler KJ (2013): Disrupted amygdala-prefrontal functional connectivity in civilian women with posttraumatic stress disorder. J Psychiatr Res 47:1469–1478.
33. Stevens JS, Kim YJ, Galatzer-Levy IR, Reddy R, Ely TD, Nemeroff CB, *et al.* (2017): Amygdala reactivity and anterior cingulate habituation predict posttraumatic stress disorder symptom maintenance after acute civilian trauma. Biol Psychiatry 81:1023–1029.
34. Koch SBJ, Van Zuiden M, Nawijn L, Frijling JL, Veltman DJ, Olff M (2017): Decreased uncinate fasciculus tract integrity in male and female patients with PTSD: A diffusion tensor imaging study. J Psychiatry Neurosci 42:331–342.
35. Dennis EL, Disner SG, Fani N, Salminen LE, Logue M, Clarke EK, *et al.* (2021): Altered white matter microstructural organization in posttraumatic stress disorder across 3047 adults: Results from the PGC-ENIGMA PTSD consortium. Mol Psychiatry 26:4315–4330.
36. Fani N, King TZ, Brewster R, Srivastava A, Stevens JS, Glover EM, *et al.* (2015): Fear-potentiated startle during extinction is associated with white matter microstructure and functional connectivity. Cortex 64:249–259.
37. Fani N, Michopoulos V, Van Rooij SJH, Clendinen C, Hardy RA, Jovanovic T, *et al.* (2019): Structural connectivity and risk for anhedonia after trauma: A prospective study and replication. J Psychiatr Res 116:34–41.
38. Fani N, King TZ, Jovanovic T, Glover EM, Bradley B, Choi K, *et al.* (2012): White matter integrity in highly traumatized adults with and without post-traumatic stress disorder. Neuropsychopharmacology 37:2740–2746.
39. Blevins CA, Weathers FW, Davis MT, Witte TK, Domino JL (2015): The posttraumatic stress disorder checklist for DSM-5 (PCL-5): Development and initial psychometric evaluation. J Trauma Stress 28:489–498.

40. Blanchard EB, Hickling EJ, Vollmer AJ, Loos WR, Buckley TC, Jaccard J (1995): Short-term follow-up of post-traumatic stress symptoms in motor vehicle accident victims. Behav Res Ther 33:369–377.
41. Broderick JE, DeWitt EM, Rothrock N, Crane PK, Forrest CB (2013): Advances in patient-reported outcomes: The NIH PROMIS(®) measures. EGEMS (Wash DC) 1:1015.
42. Rung Wu J, Chen X, Iwanaga K, Bezyak J, Rumrill S, Lee D, Chan F (2024): Psychometric validation of the PROMIS social support scale in a sample of individuals with chronic health conditions and disabilities: A factor analytic study. Rehabil Couns Bull 68:37–46.
43. Stevens JS, van Rooij SJH, Stenson AF, Ely TD, Powers A, Clifford A, *et al.* (2023): Amygdala responses to threat in violence-exposed children depend on trauma context and maternal caregiving. Dev Psychopathol 35:1159–1170.
44. Adolphs R (2008): Fear, faces, and the human amygdala. Curr Opin Neurobiol 18:166–172.
45. Shin LM, Wright CI, Cannistraro PA, Wedig MM, McMullin K, Martis B, *et al.* (2005): A functional magnetic resonance imaging study of amygdala and medial prefrontal cortex responses to overtly presented fearful faces in posttraumatic stress disorder. Arch Gen Psychiatry 62:273–281.
46. Akiki TJ, Averill CL, Abdallah CG (2017): A network-based neurobiological model of PTSD: Evidence from structural and functional neuroimaging studies. Curr Psychiatry Rep 19:81.
47. Alexander L, Clarke HF, Roberts AC (2019): A focus on the functions of Area 25. Brain Sci 9:129.
48. Kennis M, Rademaker AR, Van Rooij SJH, Kahn RS, Geuze E (2015): Resting state functional connectivity of the anterior cingulate cortex in veterans with and without post-traumatic stress disorder. Hum Brain Mapp 36:99–109.
49. Brown VM, LaBar KS, Haswell CC, Gold AL, Mid-Atlantic MIRECC Workgroup, McCarthy G, Morey RA (2014): Altered resting-state functional connectivity of basolateral and centromedial amygdala complexes in posttraumatic stress disorder. Neuropsychopharmacology 39:351–359.
50. Hammers A, Allom R, Koepp MJ, Free SL, Myers R, Lemieux L, *et al.* (2003): Three-dimensional maximum probability atlas of the human brain, with particular reference to the temporal lobe. Hum Brain Mapp 19:224–247.
51. Maldjian JA, Laurienti PJ, Kraft RA, Burdette JH (2003): An automated method for neuroanatomic and cytoarchitectonic atlas-based interrogation of fMRI data sets. Neuroimage 19:1233–1239.
52. Tyszka JM, Pauli WM (2016): In vivo delineation of subdivisions of the human amygdaloid complex in a high-resolution group template. Hum Brain Mapp 37:3979–3998.
53. Makris N, Goldstein JM, Kennedy D, Hodge SM, Caviness VS, Faraone SV, *et al.* (2006): Decreased volume of left and total anterior insular lobule in schizophrenia. Schizophr Res 83:155–171.
54. Woo C-W, Krishnan A, Wager TD (2014): Cluster-extent based thresholding in fMRI analyses: Pitfalls and recommendations. Neuroimage 91:412–419.
55. Chumbley JR, Friston KJ (2009): False discovery rate revisited: FDR and topological inference using Gaussian random fields. Neuroimage 44:62–70.
56. Genovese CR, Lazar NA, Nichols T (2002): Thresholding of statistical maps in functional neuroimaging using the false discovery rate. Neuroimage 15:870–878.
57. Whitfield-Gabrieli S, Nieto-Castanon A (2012): Conn: A functional connectivity toolbox for correlated and anticorrelated brain networks. Brain Connect 2:125–141.
58. Teipel SJ, Bokde ALW, Meindl T, Amaro E, Soldner J, Reiser MF, *et al.* (2010): White matter microstructure underlying default mode network connectivity in the human brain. Neuroimage 49:2021–2032.
59. Wakana S, Caprihan A, Panzenboeck MM, Fallon JH, Perry M, Gollub RL, *et al.* (2007): Reproducibility of quantitative tractography methods applied to cerebral white matter. Neuroimage 36:630–644.
60. Hua K, Zhang J, Wakana S, Jiang H, Li X, Reich DS, *et al.* (2008): Tract probability maps in stereotaxic spaces: Analyses of white matter anatomy and tract-specific quantification. Neuroimage 39:336–347.
61. Wade D, Varker T, Kartal D, Hetrick S, O'Donnell M, Forbes D (2016): Gender difference in outcomes following trauma-focused interventions for posttraumatic stress disorder: Systematic review and meta-analysis. Psychol Trauma 8:356–364.
62. Haider AH, Weygandt PL, Bentley JM, Monn MF, Rehman KA, Zarzaur BL, *et al.* (2013): Disparities in trauma care and outcomes in the United States: A systematic review and meta-analysis. J Trauma Acute Care Surg 74:1195–1205.
63. Memarzia J, Walker J, Meiser-Stedman R (2021): Psychological peritraumatic risk factors for post-traumatic stress disorder in children and adolescents: A meta-analytic review. J Affect Disord 282:1036–1047.
64. Knopp K, Wrape ER, McInnis R, Khalifian CE, Rashkovsky K, Glynn SM, Morland LA (2022): Posttraumatic stress disorder and relationship functioning: Examining gender differences in treatment-seeking veteran couples. J Trauma Stress 35:484–495.
65. Applebaum AJ, Stein EM, Lord-Bessen J, Pessin H, Rosenfeld B, Breitbart W (2014): Optimism, social support, and mental health outcomes in patients with advanced cancer. Psychooncology 23:299–306.
66. Li F, Luo S, Mu W, Li Y, Ye L, Zheng X, *et al.* (2021): Effects of sources of social support and resilience on the mental health of different age groups during the COVID-19 pandemic. BMC Psychiatry 21:16.
67. Beehr TA, McGrath JE (1992): Social support, occupational stress and anxiety. Anxiety Stress and Coping 5:7–19.
68. Sippel LM, Pietrzak RH, Charney DS, Mayes LC, Southwick SM (2015): How does social support enhance resilience in the trauma-exposed individual? Ecol Soc 20:1–10.
69. Ditzen B, Neumann ID, Bodenmann G, von Dawans B, Turner RA, Ehlert U, Heinrichs M (2007): Effects of different kinds of couple interaction on cortisol and heart rate responses to stress in women. Psychoneuroendocrinology 32:565–574.
70. Taylor SE, Burklund LJ, Eisenberger NI, Lehman BJ, Hilmert CJ, Lieberman MD (2008): Neural bases of moderation of cortisol stress responses by psychosocial resources. J Pers Soc Psychol 95:197–211.
71. Harandi TF, Taghinasab MM, Nayeri TD (2017): The correlation of social support with mental health. A meta-analysis. Electron Physician 9:5212–5222.
72. Reblin M, Uchino BN (2008): Social and emotional support and its implication for health. Curr Opin Psychiatry 21:201–205.
73. Paykel ES (1994): Life events, Social support and depression. Acta Psychiatr Scand Suppl 377:50–58.
74. Sherin JE, Nemeroff CB (2011): Post-traumatic stress disorder: The neurobiological impact of psychological trauma. Dialogues Clin Neurosci 13:263–278.
75. Samuelson KW (2011): Post-traumatic stress disorder and declarative memory functioning: A review. Dialogues Clin Neurosci 13:346–351.
76. Sato W, Kochiyama T, Uono S, Sawada R, Yoshikawa S (2020): Amygdala activity related to perceived social support. Sci Rep 10:2951.
77. Hyde LW, Gorka A, Manuck SB, Hariri AR (2011): Perceived social support moderates the link between threat-related amygdala reactivity and trait anxiety. Neuropsychologia 49:651–656.
78. Hornstein EA, Leschak CJ, Parrish MH, Byrne-Haltom KE, Fanselow MS, Craske MG, Eisenberger NI (2024): Social support and fear-inhibition: An examination of underlying neural mechanisms. Soc Cogn Affect Neurosci 19:nsae002.
79. Callaghan BL, Gee DG, Gabard-Durnam L, Telzer EH, Humphreys KL, Goff B, *et al.* (2019): Decreased amygdala reactivity to parent cues protects against anxiety following early adversity: An examination across 3 years. Biol Psychiatry Cogn Neurosci Neuroimaging 4:664–671.
80. Von Der Heide RJ, Skipper LM, Klobusicky E, Olson IR (2013): Dissecting the uncinate fasciculus: Disorders, controversies and a hypothesis. Brain 136:1692–1707.
81. Tottenham N, Hare TA, Casey BJ (2011): Behavioral assessment of emotion discrimination, emotion regulation, and cognitive control in childhood, adolescence, and adulthood. Front Psychol 2:39.

82. Olson IR, Plotzker A, Ezzyat Y (2007): The Enigmatic temporal pole: A review of findings on social and emotional processing. Brain 130:1718–1731.
83. Papagno C, Miracapillo C, Casarotti A, Romero Lauro LJ, Castellano A, Falini A, *et al.* (2011): What is the role of the uncinate fasciculus? Surgical removal and proper name retrieval. Brain 134:405–414.
84. Fani N, King TZ, Clendinen C, Hardy RA, Surapaneni S, Blair JR, *et al.* (2019): Attentional control abnormalities in posttraumatic stress disorder: Functional, behavioral, and structural correlates. J Affect Disord 253:343–351.
85. Harnett NG, Ference EW, Knight AJ, Knight DC (2020): White matter microstructure varies with post-traumatic stress severity following medical trauma. Brain Imaging Behav 14:1012–1024.
86. Satpute AB, Lindquist KA (2019): The default mode network's role in discrete emotion. Trends Cogn Sci 23:851–864.
87. Leech R, Braga R, Sharp DJ (2012): Echoes of the brain within the posterior cingulate cortex. J Neurosci 32:215–222.
88. Wang RWY, Chang W-L, Chuang S-W, Liu I-N (2019): Posterior cingulate cortex can be a regulatory modulator of the default mode network in task-negative state. Sci Rep 9:7565.
89. Hayden BY, Nair AC, McCoy AN, Platt ML (2008): Posterior cingulate cortex mediates outcome-contingent allocation of behavior. Neuron 60:19–25.
90. Lanius RA, Frewen PA, Tursich M, Jetly R, McKinnon MC (2015): Restoring large-scale brain networks in PTSD and related disorders: A proposal for neuroscientifically-informed treatment interventions. Eur J Psychotraumatol 6:27313.
91. Bluhm RL, Williamson PC, Osuch EA, Frewen PA, Stevens TK, Boksman K, *et al.* (2009): Alterations in default network connectivity in posttraumatic stress disorder related to early-life trauma. J Psychiatry Neurosci 34:187–194.
92. Daniels JK, McFarlane AC, Bluhm RL, Moores KA, Clark CR, Shaw ME, *et al.* (2010): Switching between executive and default mode networks in posttraumatic stress disorder: Alterations in functional connectivity. J Psychiatry Neurosci 35:258–266.
93. Whitfield-Gabrieli S, Ford JM (2012): Default mode network activity and connectivity in psychopathology. Annu Rev Clin Psychol 8:49–76.
94. Akiki TJ, Averill CL, Wrocklage KM, Scott JC, Averill LA, Schweinsburg B, *et al.* (2018): Default mode network abnormalities in posttraumatic stress disorder: A novel network-restricted topology approach. Neuroimage 176:489–498.
95. DiGangi JA, Tadayyon A, Fitzgerald DA, Rabinak CA, Kennedy A, Klumpp H, *et al.* (2016): Reduced default mode network connectivity following combat trauma. Neurosci Lett 615:37–43.
96. Geuze E, Vermetten E, de Kloet CS, Westenberg HGM (2008): Precuneal activity during encoding in veterans with posttraumatic stress disorder. Prog Brain Res 167:293–297.
97. Sippel LM, Holtzheimer PE, Huckins JF, Collier E, Feilong M, Wheatley T, Meyer ML (2021): Neurocognitive mechanisms of poor social connection in posttraumatic stress disorder: Evidence for abnormalities in social working memory. Depress Anxiety 38:615–625.
98. Pei R, Courtney AL, Ferguson I, Brennan C, Zaki J (2023): A neural signature of social support mitigates negative emotion. Sci Rep 13:17293.
99. Maresh EL, Beckes L, Coan JA (2013): The social regulation of threat-related attentional disengagement in highly anxious individuals. Front Hum Neurosci 7:515.
100. Coan JA, Beckes L, Gonzalez MZ, Maresh EL, Brown CL, Hasselmo K (2017): Relationship status and perceived support in the social regulation of neural responses to threat. Soc Cogn Affect Neurosci 12:1574–1583.
101. Van Den Heuvel M, Mandl R, Luigjes J, Hulshoff Pol H (2008): Microstructural organization of the cingulum tract and the level of default mode functional connectivity. J Neurosci 28:10844–10851.
102. Bubb EJ, Metzler-Baddeley C, Aggleton JP (2018): The cingulum bundle: Anatomy, function, and dysfunction. Neurosci Biobehav Rev 92:104–127.
103. Fransson P, Marrelec G (2008): The precuneus/posterior cingulate cortex plays a pivotal role in the default mode network: Evidence from a partial correlation network analysis. Neuroimage 42:1178–1184.
104. Leech R, Sharp DJ (2014): The role of the posterior cingulate cortex in cognition and disease. Brain 137:12–32.
105. Daniels JK, Lamke J-P, Gaebler M, Walter H, Scheel M (2013): White matter integrity and its relationship to PTSD and childhood TRAUMA-A systematic review and meta-analysis. Depress Anxiety 30:207–216.
106. Kennis M, Van Rooij SJH, Tromp DPM, Fox AS, Rademaker AR, Kahn RS, *et al.* (2015): Treatment outcome-related white matter differences in veterans with posttraumatic stress disorder. Neuropsychopharmacology 40:2434–2442.
107. Kennis M, van Rooij SJH, Reijnen A, Geuze E (2017): The predictive value of dorsal cingulate activity and fractional anisotropy on long-term PTSD symptom severity. Depress Anxiety 34:410–418.
108. Wu Q, Huang Q, Liu C, Wu H (2023): Oxytocin modulates social brain network correlations in resting and task state. Cereb Cortex 33:3607–3620.
109. Uchino BN, Trettevik R, Kent de Grey RG, Cronan S, Hogan J, Baucom BRW (2018): Social support, social integration, and inflammatory cytokines: A meta-analysis. Health Psychol 37:462–471.
110. Yang YC, Schorpp K, Harris KM (2014): Social support, social strain and inflammation: Evidence from a national longitudinal study of U.S. adults. Soc Sci Med 107:124–135.

SUPPLEMENTARY INFORMATION

Social Buffering of Posttraumatic Stress Disorder: Longitudinal Effects and Neural Mediators

Santos *et al.*

Supplemental Materials

Methods

T1-weighted anatomical imaging

High resolution anatomical imaging data was collected from T1-weighted structural scans to assess morphology of brain regions that may be predictive of posttraumatic outcomes and allow longitudinal assessment of brain structure over time. Anatomical images were collected using a multi-echo magnetization prepared rapid acquisition gradient echo (ME-MPRAGE). ME-MPRAGE images were collected with consistent parameters across imaging sites at a 1mm isotropic resolution. However, one imaging site was not able to use the SIEMENS ME-MPRAGE sequence and conducted a standard 1mm isotropic MPRAGE sequence instead.

Image Visualization

DICOM images were converted to NIFTI format with Brain Imaging Data Structure (BIDS) nomenclature using dcm2niix (1) and were visually inspected for conversion errors and data exclusion criteria (e.g., signal drop-out from Falx calcification, anatomical abnormalities). Further quality control was achieved by running the MRIQC pipeline (version 0.10.4 in a Docker container) (2) on the structural and functional images.

Functional data preprocessing and statistical modeling

Results included in this manuscript come from preprocessing performed using fMRIPrep 1.2.2 ((3); (4); RRID:SCR_016216), which is based on Nipype 1.1.5 ((5); (6); RRID:SCR_002502). To maintain consistency in preprocessing throughout the duration of data collection, FMRIPrep was run in a Docker container retaining the version that was newest at the initiation of the study.

For each of the 4 BOLD runs found per subject (across all tasks and sessions), the following preprocessing was performed. First, a reference volume and its skull-stripped version were generated using a custom methodology of fMRIPrep. The BOLD reference was then co-registered to the T1w reference using bbregister (FreeSurfer) which implements boundary-based

registration (7). Co-registration was configured with nine degrees of freedom to account for distortions remaining in the BOLD reference. Head-motion parameters with respect to the BOLD reference (transformation matrices, and six corresponding rotation and translation parameters) are estimated before any spatiotemporal filtering using mcflirt (FSL 5.0.9, (8)). BOLD runs were slice-time corrected using 3dTshift from AFNI 20160207 ((9), RRID:SCR_005927). The BOLD time-series (including slice-timing correction) were resampled onto their original, native space by applying a single, composite transform to correct for head-motion and susceptibility distortions. These resampled BOLD time-series will be referred to as ‘preprocessed BOLD in original space’, or just ‘preprocessed BOLD.’ First, a reference volume and its skull-stripped version were generated using a custom methodology of fMRIPrep. Automatic removal of motion artifacts using independent component analysis (ICA-AROMA, (10)) was performed on the preprocessed BOLD on MNI space time-series after removal of non-steady state volumes and spatial smoothing with an isotropic, Gaussian kernel of 6mm FWHM (full-width half-maximum). Corresponding "non-aggressively" denoised runs were produced after such smoothing. To deal with cases in which motion was likely too high for effective ICA-based correction, we also implemented an overall motion threshold was set such that data from a particular task (Threat, Inhibition, Reward, Resting State) were excluded from analysis entirely for any participant with more than 15% of volumes exceeding 1mm FD.

Additionally, the "aggressive" noise-regressors were collected and placed in the corresponding confounds file. Although not used in our current analyses, these regressors and corresponding non-denoised and unsmoothed images are available for alternative analyses in the future. These noise regressors were generated as follows: The BOLD time-series were resampled to MNI152NLin2009cAsym standard space, generating a preprocessed BOLD run in MNI152NLin2009cAsym space. First, a reference volume and its skull-stripped version were generated using a custom methodology of fMRIPrep. Several confounding time-series were

calculated based on the preprocessed BOLD: framewise displacement (FD), DVARS and three region-wise global signals. FD and DVARS are calculated for each functional run, both using their implementations in Nipype (following definitions by Powers et al. 2012 (11)). The three global signals are extracted within the CSF, the WM, and the whole-brain masks.

The BOLD time-series were resampled to surfaces on the following spaces: fsaverage5. All resamplings can be performed with a single interpolation step by composing all the pertinent transformations (i.e. head-motion transform matrices, susceptibility distortion correction when available, and co-registrations to anatomical and template spaces). Gridded (volumetric) resampling was performed using antsApplyTransforms (ANTs), configured with Lanczos interpolation to minimize the smoothing effects of other kernels (12). Non-gridded (surface) resampling was performed using `mri_vol2surf`(FreeSurfer). Many internal operations of fMRIPrep use Nilearn 0.4.2 ((13), RRID:SCR_001362), mostly within the functional processing workflow.

Through statistical parametric mapping software (SPM12), a first-level general linear model was fitted for individual subjects' neuroimaging data.

Diffusion-weighted imaging preprocessing and statistical modeling

DWI data were processed similarly to prior published methods. The non-weighted DWI volumes were motion corrected and averaged to serve as a reference for further processing. Motion and eddy current effects in the DWI data were reduced using the 'eddy' subroutine in FSL (version 6.0) to match the diffusion weighted volumes to the average non-weighted volume ((14); (15)). Susceptibility effects were corrected for using nonlinear warping of the DWI data to the participant's T1-weighted anatomical scan (16). T1-weighted images were skull-stripped using the Robust Brain Extraction (ROBEX) tool (17) and were then contrast inverted to match the averaged non-weighted volume. Nonlinear warping was completed through the Symmetric Normalization (SyN) routine in the Advanced Normalization Tools (ANTs) suite (18). SyN was first

used to warp the averaged non-weighted volume to the anatomical image, and the resulting warp parameters were applied to the full DWI data. DWI data were then downsampled to a 2mm isotropic grid-spacing and fit with a tensor model (FMRIB Diffusion Toolbox). Tract-Based Spatial Statistics (TBSS) processing was used as implemented in the ENIGMA-DTI working group processing standards to extract FA values across white matter regions (19, 20). First, FA maps were non-linearly registered to the standard ENIGMA FA map in Montreal Neurological Institute (MNI) standard space (19). The ENIGMA FA skeleton map was then projected onto each subjects FA maps in standard space. Finally, regional FA values were extracted from the JHU White matter atlas and used in group level analyses (21-23).

DWI data were subject to several levels of quality control. Raw DWI data were initially visually inspected for artefacts that diminish data quality (e.g., slice-wise signal loss, movement artefacts, ghosting, etc.). Further, image quality metrics are extracted for the raw data to provide a numeric metric of potential diminishments of data quality and to assess the potential impact of artefacts observed during visual inspection utilizing prior published methods and freely available scripts. Additional quality control metrics were extracted using the QUAD subroutine in FSL following motion and eddy current correction to derive metrics of participant motion, eddy current distortion, and other quality metrics. We further performed visual quality control of the processed DTI and TBSS data using the quality control procedures outlined by the ENIGMA-DTI working group. Visual inspection was performed following tensor fitting to confirm the FA and principal eigenvector maps were correctly aligned. Visual inspection was also performed to confirm proper alignment between ENIGMA white matter skeleton and individual participant FA maps with calculation of distance metrics of the projection to ensure goodness of fit.

Supplemental Tables and Figures

Table S1a: Effect of 2-Week emotional support on 6-Month PTSD symptom severity (MVC only, n=197)*				
	Beta	**SE**	***t***	***p***
2 Week PROMIS Scores	**-0.162**	**0.077**	**-2.110**	**0.037**
Sex/Gender (assigned at birth)	**0.204**	**0.079**	**2.577**	**0.011**
Ethnic/Racial Identity	**-0.040**	**0.081**	**-0.492**	**0.624**
Trauma Severity	**0.041**	**0.081**	**0.513**	**0.609**
Neuroimaging Site	**0.018**	**0.077**	**0.239**	**0.812**
Age	**0.067**	**0.077**	**0.873**	**0.384**

**Covariates included sex, ethnic/racial identity, trauma severity, age and site*

Table S1b: Effect of 2-Week emotional support on 6-Month PTSD symptom severity (Non-MVC only, n=80)				
	Beta	**SE**	***t***	***p***
2 Week PROMIS Scores	**-0.051**	**0.116**	**-0.436**	**0.665**
Sex/Gender (assigned at birth)	**-0.056**	**0.124**	**-0.453**	**0.653**
Ethnic/Racial Identity	**0.054**	**0.146**	**0.372**	**0.712**
Trauma Severity	**0.041**	**0.119**	**0.346**	**0.731**
Neuroimaging Site	**-0.084**	**0.136**	**-0.618**	**0.539**
Age	**0.277**	**0.123**	**2.248**	**0.029**

Table S2a: Effects of 2-week emotional support on threat reactivity (Fearful>Neutral) in *a priori* ROIs*

	Beta	SE	t	p - values	FDR corrected p-value
Left Amygdala	-0.009	0.059	-0.145	0.885	0.885
Right Amygdala	-0.021	0.058	-0.360	0.719	0.885
Left Hippocampus	0.015	0.058	0.264	0.792	0.885
Right Hippocampus	0.059	0.059	1.009	0.314	0.885
Left Insula	-0.010	0.059	-0.164	0.869	0.885
Right Insula	0.022	0.059	0.368	0.713	0.885
Brodmann's Area 32	0.029	0.060	0.490	0.624	0.885
Brodmann's Area 25	0.097	0.060	1.631	0.104	0.832

**Covariates included sex, ethnic/racial identity, trauma severity, age and site*

Table S2b: Effects of 2-week emotional support on threat reactivity (Fearful>Neutral) in *a priori* ROIs, without covariates*

	Beta	SE	t	p - values	FDR corrected p-value
Left Amygdala	-1.64E-05	0.003	-0.005	0.996	0.996
Right Amygdala	-0.001	0.003	-0.337	0.736	0.993
Left Hippocampus	0.001	0.003	0.326	0.745	0.993
Right Hippocampus	0.003	0.003	1.031	0.303	0.993
Left Insula	0.0002	0.003	0.051	0.959	0.996
Right Insula	0.002	0.004	0.478	0.633	0.993
Brodmann's Area 32	0.002	0.003	0.613	0.541	0.993
Brodmann's Area 25	0.005	0.003	1.572	0.117	0.936

Table S3: Effect of 2-week emotional support on *a priori* white matter tracts, without covariates					
	Beta	**SE**	***t***	***p*-values**	***FDR corrected p-value***
2-Week Emotional Support					
Bilateral Cingulum (Cingulate Gyrus)	0.148	0.063	2.356	0.019	0.019
Bilateral Cingulum (Hippocampus)	-0.022	0.062	-0.347	0.729	0.729
Bilateral Uncinate Fasciculus	0.156	0.063	2.466	0.014	0.014

Figure S1 – *Brain regions engaged in response to social threat cues: Fearful > Neutral contrast*

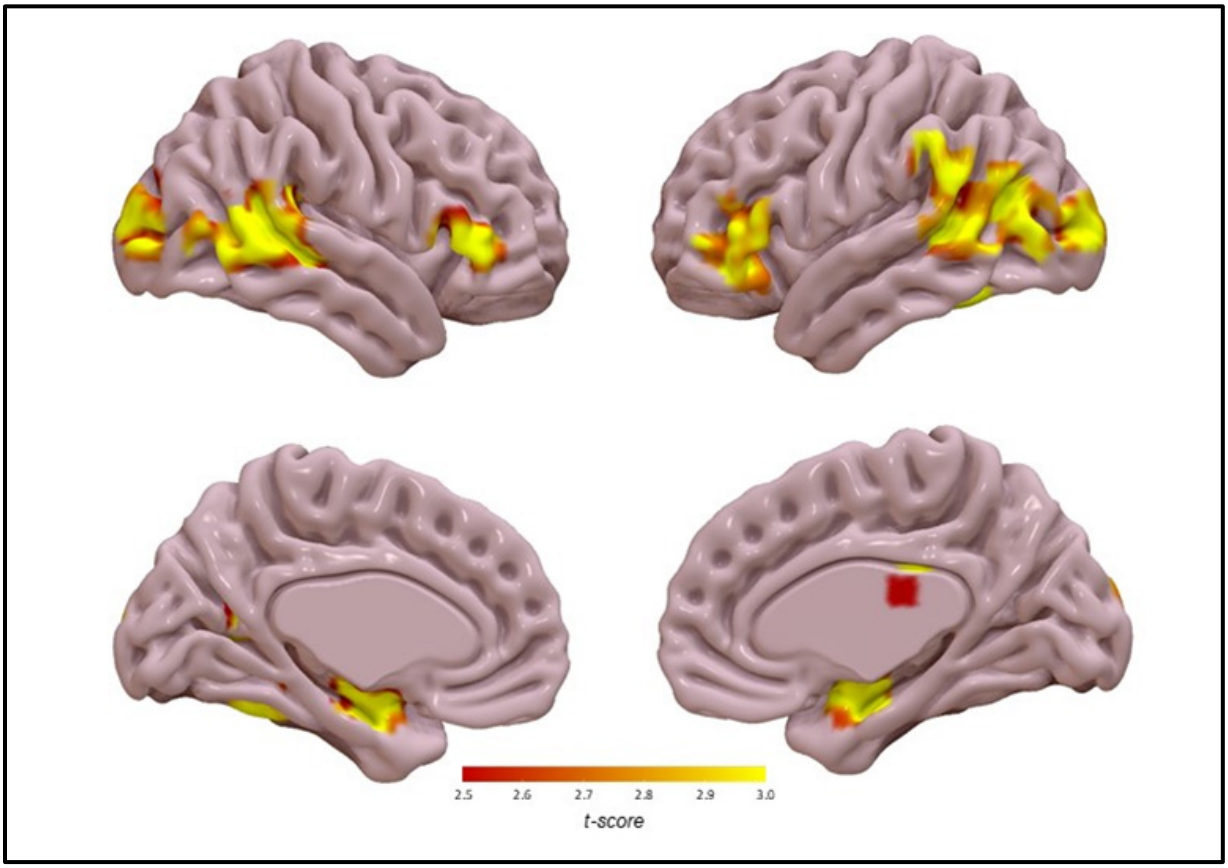

Supplemental References

1. Li X, Morgan PS, Ashburner J, Smith J, Rorden C. The first step for neuroimaging data analysis: DICOM to NIfTI conversion. Journal of Neuroscience Methods. 2016;264:47-56. doi: 10.1016/j.jneumeth.2016.03.001.
2. Esteban O, Birman D, Schaer M, Koyejo OO, Poldrack RA, Gorgolewski KJ. MRIQC: Advancing the automatic prediction of image quality in MRI from unseen sites. PLOS ONE. 2017;12(9):e0184661. doi: 10.1371/journal.pone.0184661.
3. Esteban O, Blair R, Markiewicz C, Berleant S, Moodie C, Ma F, et al. poldracklab/fmriprep: 1.0. 0-rc5 (Version 1.0. 0-rc5). Zenedo. 2017.
4. Esteban O, Markiewicz CJ, Blair RW, Moodie CA, Isik AI, Erramuzpe A, et al. fMRIPrep: a robust preprocessing pipeline for functional MRI. Nature Methods. 2019;16(1):111-6. doi: 10.1038/s41592-018-0235-4.
5. Gorgolewski K, Burns CD, Madison C, Clark D, Halchenko YO, Waskom ML, et al. Nipype: A Flexible, Lightweight and Extensible Neuroimaging Data Processing Framework in Python. Frontiers in Neuroinformatics. 2011;5. doi: 10.3389/fninf.2011.00013.
6. Gorgolewski K, Esteban O, Ellis D, Notter M, Ziegler E, Johnson H, et al. Nipype: A flexible, lightweight and extensible neuroimaging data processing framework in Python. Zenodo. 2017.
7. Greve DN, Fischl B. Accurate and robust brain image alignment using boundary-based registration. Neuroimage. 2009;48(1):63-72. Epub 20090630. doi: 10.1016/j.neuroimage.2009.06.060. PubMed PMID: 19573611; PubMed Central PMCID: PMC2733527.
8. Jenkinson M, Bannister P, Brady M, Smith S. Improved optimization for the robust and accurate linear registration and motion correction of brain images. Neuroimage. 2002;17(2):825-41. doi: 10.1016/s1053-8119(02)91132-8. PubMed PMID: 12377157.
9. Cox RW. AFNI: Software for Analysis and Visualization of Functional Magnetic Resonance Neuroimages. Computers and Biomedical Research. 1996;29(3):162-73. doi: 10.1006/cbmr.1996.0014.
10. Pruim RHR, Mennes M, van Rooij D, Llera A, Buitelaar JK, Beckmann CF. ICA-AROMA: A robust ICA-based strategy for removing motion artifacts from fMRI data. Neuroimage. 2015;112:267-77. Epub 20150311. doi: 10.1016/j.neuroimage.2015.02.064. PubMed PMID: 25770991.
11. Power JD, Barnes KA, Snyder AZ, Schlaggar BL, Petersen SE. Spurious but systematic correlations in functional connectivity MRI networks arise from subject motion. NeuroImage. 2012;59(3):2142-54. doi: 10.1016/j.neuroimage.2011.10.018.
12. Lanczos C. A Precision Approximation of the Gamma Function. Journal of the Society for Industrial and Applied Mathematics Series B Numerical Analysis. 1964;1(1):86-96. doi: 10.1137/0701008.
13. Abraham A, Pedregosa F, Eickenberg M, Gervais P, Mueller A, Kossaifi J, et al. Machine learning for neuroimaging with scikit-learn. Frontiers in Neuroinformatics. 2014;8. doi: 10.3389/fninf.2014.00014.
14. Andersson JLR, Sotiropoulos SN. An integrated approach to correction for off-resonance effects and subject movement in diffusion MR imaging. Neuroimage. 2016;125:1063-78. Epub 20151020. doi: 10.1016/j.neuroimage.2015.10.019. PubMed PMID: 26481672; PubMed Central PMCID: PMC4692656.
15. Smith SM, Jenkinson M, Woolrich MW, Beckmann CF, Behrens TEJ, Johansen-Berg H, et al. Advances in functional and structural MR image analysis and implementation as FSL. NeuroImage. 2004;23:S208-S19. doi: 10.1016/j.neuroimage.2004.07.051.

16. Wang S, Peterson DJ, Gatenby JC, Li W, Grabowski TJ, Madhyastha TM. Evaluation of Field Map and Nonlinear Registration Methods for Correction of Susceptibility Artifacts in Diffusion MRI. Frontiers in Neuroinformatics. 2017;11. doi: 10.3389/fninf.2017.00017.
17. Iglesias JE, Liu CY, Thompson PM, Tu Z. Robust Brain Extraction Across Datasets and Comparison With Publicly Available Methods. IEEE Transactions on Medical Imaging. 2011;30(9):1617-34. doi: 10.1109/TMI.2011.2138152.
18. Avants BB, Tustison NJ, Song G, Cook PA, Klein A, Gee JC. A reproducible evaluation of ANTs similarity metric performance in brain image registration. Neuroimage. 2011;54(3):2033-44. Epub 20100917. doi: 10.1016/j.neuroimage.2010.09.025. PubMed PMID: 20851191; PubMed Central PMCID: PMC3065962.
19. Jahanshad N, Kochunov PV, Sprooten E, Mandl RC, Nichols TE, Almasy L, et al. Multi-site genetic analysis of diffusion images and voxelwise heritability analysis: A pilot project of the ENIGMA–DTI working group. NeuroImage. 2013;81:455-69. doi: https://doi.org/10.1016/j.neuroimage.2013.04.061.
20. Smith SM, Jenkinson M, Johansen-Berg H, Rueckert D, Nichols TE, Mackay CE, et al. Tract-based spatial statistics: Voxelwise analysis of multi-subject diffusion data. NeuroImage. 2006;31(4):1487-505. doi: https://doi.org/10.1016/j.neuroimage.2006.02.024.
21. Oishi K, Zilles K, Amunts K, Faria A, Jiang H, Li X, et al. Human brain white matter atlas: identification and assignment of common anatomical structures in superficial white matter. Neuroimage. 2008;43(3):447-57. Epub 20080718. doi: 10.1016/j.neuroimage.2008.07.009. PubMed PMID: 18692144; PubMed Central PMCID: PMC2586008.
22. MRI Atlas of Human White Matter. AJNR Am J Neuroradiol. 2006;27(6):1384-5.
23. Wakana S, Caprihan A, Panzenboeck MM, Fallon JH, Perry M, Gollub RL, et al. Reproducibility of quantitative tractography methods applied to cerebral white matter. Neuroimage. 2007;36(3):630-44. Epub 20070320. doi: 10.1016/j.neuroimage.2007.02.049. PubMed PMID: 17481925; PubMed Central PMCID: PMC2350213.